Differential Effects of Amino-Terminal Distal and Proximal Domains in the Regulation of Human *erg* K^+ Channel Gating

Cristina G. Viloria, Francisco Barros, Teresa Giráldez, David Gómez-Varela, and Pilar de la Peña
Departamento de Bioquímica y Biología Molecular, Facultad de Medicina, C/J Clavería s/n, Universidad de Oviedo, E-33006 Oviedo, Spain

ABSTRACT The participation of amino-terminal domains in human *ether-a-go-go* (*eag*)-*related* gene (HERG) K^+ channel gating was studied using deleted channel variants expressed in *Xenopus* oocytes. Selective deletion of the HERG-specific sequence (HERG Δ138–373) located between the conserved initial amino terminus (the *eag* or PAS domain) and the first transmembrane helix accelerates channel activation and shifts its voltage dependence to hyperpolarized values. However, deactivation time constants from fully activated states and channel inactivation remain almost unaltered after the deletion. The deletion effects are equally manifested in channel variants lacking inactivation. The characteristics of constructs lacking only about half of the HERG-specific domain (Δ223–373) or a short stretch of 19 residues (Δ355–373) suggest that the role of this domain is not related exclusively to its length, but also to the presence of specific sequences near the channel core. Deletion-induced effects are partially reversed by the additional elimination of the *eag* domain. Thus the particular combination of HERG-specific and *eag* domains determines two important HERG features: the slow activation essential for neuronal spike-frequency adaptation and maintenance of the cardiac action potential plateau, and the slow deactivation contributing to HERG inward rectification.

INTRODUCTION

The human-*ether-a-go-go* related gene (h-*erg*) encodes a potassium channel (HERG) that mediates the cardiac repolarizing current I_{Kr} (Sanguinetti et al., 1995; Trudeau et al., 1995). The physiological importance of HERG is emphasized by the discovery of certain forms of familial long-QT syndrome linked to mutations in the h-*erg* gene (Curran et al., 1995; Sanguinetti et al., 1995; Spector et al., 1996a). HERG channels are also molecular targets for widely used pharmacological agents such as class III antiarrhythmics (Spector et al., 1996a), antipsychotic drugs (Suessbrich et al., 1997a), histamine receptor antagonists (Suessbrich et al., 1996; Taglialatela et al., 1998), calcium channel blockers (Chouabe et al., 1998), and sulfonylurea antidiabetic drugs (Rosati et al., 1998). Furthermore, they have been implicated in changes in resting membrane potential associated with the cell cycle, in the control of neuritogenesis and differentiation in neuronal cells, and in the spike-frequency accommodation of neuronal firing (Arcangeli et al., 1993, 1995; Faravelli et al., 1996; Chiesa et al., 1997; Schönherr et al., 1999). Finally, mutations in the *erg* gene of *Drosophila* produce neurological defects (Titus et al., 1997; X. Wang et al., 1997), and the rat counterpart of HERG constitutes an important target for the control of electrical activity and hence for the modulation of neurosecretion in adenohypophysial cells (Barros et al., 1994, 1997; Schäfer et al., 1999).

The time and voltage dependencies of HERG currents determine their role in the regulation of cell excitability. This includes a slow activation rate that overlaps with a rapid and voltage-dependent inactivation process, limiting the level of outward current upon depolarization. At negative repolarizing voltages, prominent tail currents are produced after reopening of the channels as they rapidly recover from inactivation, before closing at quite a slow rate (Trudeau et al., 1995; Sanguinetti et al., 1995; Smith et al., 1996; Schönherr and Heinemann, 1996; Spector et al., 1996b; S. Wang et al., 1997). This makes HERG operate as an inward rectifier, although it has the six membrane-spanning domains and the S4 and the regions typical of depolarization-activated channels (Warmke and Ganetzky, 1994).

The molecular basis of HERG kinetic characteristics are not completely understood. Recent work resolving the crystal structure of the highly conserved HERG initial domain (Cabral et al., 1998) identified it as a eukaryotic PAS domain (the *eag* or PAS domain) involved in the regulation of channel gating (Cabral et al., 1998). Removal of this domain markedly increased HERG deactivation rates (Schönherr and Heinemann, 1996; Spector et al., 1996b; Wang et al., 1998; Cabral et al., 1998) by eliminating its interaction with the gating machinery, probably the S4-S5 linker (Wang et al., 1998; Cabral et al., 1998). One exclusive structural feature of HERG is the presence of a long stretch of amino acids (named here the HERG-specific or "proximal" domain by its proximity to the S1 helix and the channel core) that follows the conserved *eag* domain and extends from about position 135 to about position 366 (Warmke and Ganetzky, 1994). However, the spatial struc-

Received for publication 6 December 1999 and in final form 16 March 2000.

Address reprint requests to Dr. Pilar de la Peña, Departamento de Bioquímica y Biología Molecular, Facultad de Medicina, C/J Clavería s/n, Universidad de Oviedo, E-33006 Oviedo, Spain. Tel.: 34-985-103565; Fax: 34-985-103157; E-mail:paco@bioaxp.quimica.uniovi.es.

0006-3495/00/07/231/16 $2.00

ture and functional significance of this protein region are unknown.

The best described functional role of K^+ channel amino-terminal domains is to provide the "ball" and "chain" structures for N-type inactivation (Hoshi et al., 1990). Nevertheless, HERG inactivation takes place through a C-type mechanism not related to the amino terminus (Smith et al., 1996; Schönherr and Heinemann, 1996; Spector et al., 1996b; S. Wang et al., 1997; Wang et al., 1998). The structure of the relatively short protein domains linking the initial ball and the S1 helix in several K^+ channels has been elucidated recently (Kreusch et al., 1998; Bixby et al., 1999). However, the kind of interaction that takes place between these T1 domains and the channel core is still unknown. Furthermore, whereas the T1 domains are regarded as crucial determinants of channel assembly, HERG channels lacking almost the whole amino terminus are normally expressed in the plasma membrane (Schönherr and Heinemann, 1996; Spector et al., 1996b; Wang et al., 1998; Cabral et al., 1998).

Recent work has implicated the amino terminus of different channels, including HERG, in the regulation of voltage dependence and/or activation kinetics (Schönherr and Heinemann, 1996; Spector et al., 1996b; Terlau et al., 1997; Marten and Hoshi, 1997, 1998; Pascual et al., 1997; Chiara et al., 1999). In this report we tested the relevance of the proximal domain on HERG channel gating. We found that deletion of this domain induces a dramatic acceleration of channel activation associated with a shift in its voltage dependence. However, both deactivation from fully activated states and channel inactivation are poorly affected by the deletion. This and the results obtained with channel variants from which the *eag* domain has been also deleted lead us to propose a model in which both the long HERG-specific and the initial *eag* domains play an important role in setting HERG gating characteristics. Hence the HERG-specific proximal domain seems to constitute an important element determining the role of HERG channels in the maintenance of cell resting potential, electrical excitability, and accommodation of neuronal and cardiac firing.

MATERIALS AND METHODS

Generation of channel mutants

To construct the amino-terminal deletion mutant Δ2–370, a forward polymerase chain reaction (PCR) primer was synthesized to introduce a *Hin*dIII site, 6 bp of 5′ untranslated sequence, an ATG, and 24 bp of HERG coding sequence corresponding to amino acids 371–378 (5′-TTG AAG CTT CTC AGG ATG ACT GAG AAG GTC ACC CAG GTC CTG-3′). The reverse primer covered a unique *Xho*I site in position 2272 (amino acid 697) of the HERG sequence (5′-GAA GTA CTC CTC GAG GCG CTG GCG-3′). The corresponding PCR product was digested with *Hin*dIII and *Xho*I, gel purified, and ligated into *Hin*dIII/*Xho*I-digested wild-type HERG in the pSP64 expression vector. For the fully proximal domain-deleted mutant (Δ138–373) a forward PCR primer containing a *Hin*dIII site and covering the start codon (5′-TTG AAG CTT CTC AGG ATG CCG GTG CGG AGG GGC CAC-3′) was synthesized and used in PCR reactions with a reverse primer containing 27 bp of coding sequence corresponding to amino acids 129–137, followed by 9 bp of sequence corresponding to amino acids 374–376 and covering a unique *Bst*EII site (5′-GGA AGG TGA CCA TGT CCT TCT CCA TCA CCA CCT CGA A-3′). The partially deleted mutants Δ170–190, 223–373 and Δ186–191, 223–373 were generated in a similar way by using the same forward PCR primer (containing a *Hin*dIII site and the start codon) and a reverse primer containing 27 bp of coding sequence corresponding to amino acids 214–222, followed by a 9-bp sequence corresponding to amino acids 374–376 and covering the unique *Bst*EII site (5′-GAG GGT GAC CAC GTG GTT GTC CAT GGC TGT CAC TTC-3′). Screening of a number of clones for the Δ223–373 mutant revealed the systematic introduction of additional internal deletions in positions upstream of amino acid 223. It is probable that the presence of a region particularly enriched in G-C pairs around positions 690–760 of the HERG sequence (corresponding to amino acids 170–193) caused the consistent production of errors during the PCR reactions. Because of this, two partially deleted mutants lacking either 21 or 6 amino acids (corresponding to positions 170–190 and 186–191, respectively), besides the designed 223–373 deletion, were selected for the experiments. The small deletion mutant Δ355–373 was generated using the same forward PCR primer as above (with a *Hin*dIII site and the start codon) and a reverse primer containing 27 bp of coding sequence corresponding to amino acids 346–354, followed by a 9-bp sequence corresponding to amino acids 374–376 also covering the unique *Bst*EII site (5′-CTC GGT GAC CCT GGT GGG CGA AGC CAA GAA GGG GTC-3′). The resulting PCR products were digested with *Hin*dIII/*Bst*EII, gel purified, and ligated into *Hin*dIII/*Bst*EII-digested wild-type HERG in the pS64 vector. The point mutant S620T was created by site-directed mutagenesis, using a PCR-based overlap extension method as previously described (Ho et al., 1989). The final PCR fragment was digested with *Bst*EII and *Bgl*II and reinserted into the wild-type clone at the corresponding sites. In the constructs that combined the S620T mutation with deletions, the *Bst*EII/*Bgl*II fragment was reinserted into the deletion mutant clones at the corresponding sites. All constructs were sequenced by the dideoxy chain termination method (Sanger et al., 1977) to confirm the mutations and to ensure the absence of errors.

Plasmids and preparation of cRNA

The plasmid containing the cDNA for the HERG channel was a generous gift of Dr. E. Wanke (University of Milan, Milan, Italy). Plasmids were linearized, and capped cRNA was synthesized in vitro from the linear cDNA templates by standard methods, using SP6 RNA polymerase as described (de la Peña et al., 1992).

Oocyte expression and solutions

Procedures for frog anesthesia and surgery, obtaining oocytes, and microinjection have been detailed elsewhere (Barros et al., 1998). Oocytes were maintained in OR-2 medium (in mM: 82.5 NaCl, 2 KCl, 2 $CaCl_2$, 2 $MgCl_2$, 1 Na_2HPO_4, 10 HEPES, at pH 7.5). Cytoplasmic microinjections were performed with 30–50 nl of in vitro synthesized cRNA per oocyte. HERG currents were studied in manually defolliculated oocytes (de la Peña et al., 1992; Barros et al., 1998). Unless otherwise indicated, recordings were obtained in extracellular high-K^+ OR-2 medium in which 50 mM KCl was substituted for an equivalent amount of NaCl. Functional expression was typically assessed 2–3 days after microinjection.

Data acquisition and analysis

Recordings were made at room temperature with the two-electrode voltage-clamp method as described previously (Barros et al., 1998). Membrane

potential was typically clamped at −80 mV, and at −100 or −110 mV for Δ138–373 and Δ223–373 deleted channels. Stimulation and data acquisition were controlled with Pulse+PulseFit software (HEKA Elektronic, Lambrecht, Germany) running on Macintosh computers. Data analysis was performed with the programs PulseFit (HEKA Elektronic) and Igor-Pro (WaveMetrics, Lake Oswego, OR). A *P*/*n* method was used for leak and capacitive current subtraction. The leak holding potential was set at −100 for basal voltages of −80 and −100 mV, and at −110 mV for cells clamped at −110 mV. Usually, a scaling factor of −0.2 was used. Kinetic parameters of activation, deactivation, inactivation, and inactivation recovery were obtained as previously described (Barros et al., 1998), using the voltage protocols shown on the graphs. The amount of injected cRNA was calibrated to yield inward tail currents in the range of 1–5 μA at repolarization voltages around −100 mV to ensure proper clamp control. Fits to tail currents from inactivating channels began as soon as the clamp settled. A single-exponential function of positive amplitude was applied to the inactivation recovery phase, followed by a negative-amplitude biexponential fit to the decaying phase of the tail. Deactivation parameters for S620T noninactivating channels were obtained from double-exponential fits to the tails, with the first cursor of the fitting window located at the end of the capacitive transient. Data are presented as means ± SE; the number of oocytes is indicated by *n* and the number of frogs by *N*.

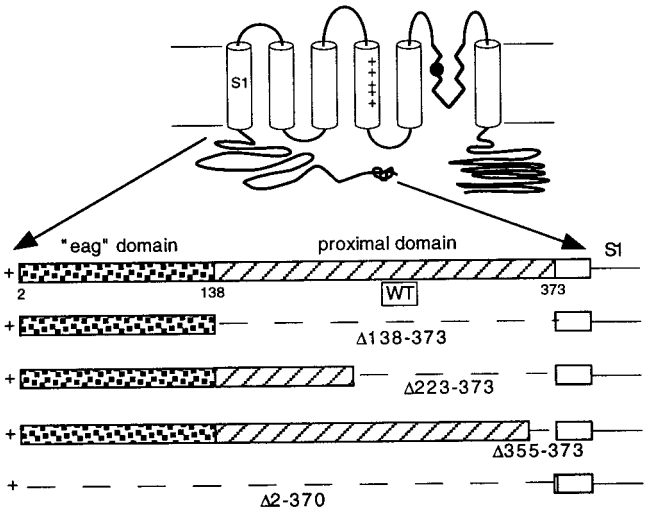

FIGURE 1 Topology of a HERG channel subunit. The transmembrane helices S1–S6 are represented by six cylinders at the top. The positions of the S1 helix, the voltage sensor in S4, and the P region between S5 and S6 are highlighted. The approximate situation of the amino acid residue subjected to point mutation in this study is also indicated by a black dot in the scheme. Schematic representations of the amino terminus in wild-type and deletion mutants are shown at the bottom. The *eag* and the proximal domains are marked by dotted and striped bars, respectively. Deletions are marked by dashed lines. The size of every domain and the lengths of the deletions are represented on a horizontal scale as proportional to the total length of the amino terminus.

RESULTS

Deletion of the HERG-specific proximal domain in the amino terminus selectively modifies activation gating

Effect of proximal domain deletion on HERG activation rates

The amino terminus of the HERG channel is composed of an initial domain (the *eag* or PAS domain; Fig. 1) conserved among all members of the *eag* family (approximately residues 2–136), followed by a long stretch of amino acids exclusive of HERG (named here as the HERG-specific or proximal domain because of its proximity to the channel core) up to residue 367, which is close to position 397, which signals the beginning of the putative first transmembrane S1 segment (Warmke and Ganetzky, 1994). To test the functional significance of the proximal domain on channel gating, we created a mutant of HERG in which residues 138–373, corresponding to the total length of this domain, were deleted (Fig. 1). The effect of the deletion on activation rates at voltages between −20 and +40 mV is illustrated in Fig. 2 and compared to those exhibited by wild-type channels. When expressed in *Xenopus* oocytes, the channels lead to small outward currents upon depolarization due to overlap of relatively slow activation and very fast inactivation, followed by big deactivation tail currents after return to negative voltages. These tails, inward under the ionic conditions used here, show an initial rising phase as a result of fast inactivation removal, followed by a slow decay due to channel closing. Because of superposition of slow activation transitions and fast inactivation rates upon depolarization, we monitored the time course of transitions from closed to open (and inactive) states, by using an indirect envelope of tail currents (Barros et al., 1998), varying the duration of the depolarization pulse, fitting the relaxation of the tail currents recorded after going back to a negative voltage, and extrapolating the magnitude of the decaying current to the moment the depolarizing pulse ended. In wild-type channels, the time required to attain a half-maximum current magnitude decreased from near 400 ms at −20 mV to ~50 ms at +40 mV (Fig. 2). The selective elimination of the proximal domain (Δ138–373) results in a channel protein with activation kinetics accelerated by almost an order of magnitude at similar voltages between −20 and +20 mV.

Effect of proximal domain deletion on HERG steady-state activation properties

During the initial experiments with HERG Δ138–373 channels, we noticed that the resting potential of oocytes expressing this variant was significantly more negative (−76 ± 1.2 mV (n = 15)) than that of oocytes expressing wild-type channels (−56 ± 1.2 (n = 19)). Furthermore, large holding currents were obtained when cells expressing Δ138–373 channels were maintained at voltages positive to −100 mV. This suggested that the Δ138–373 variant could have its voltage dependence of activation shifted to quite negative potentials.

To better understand the reasons for changes in activation, we studied the voltage dependence of the gating tran-

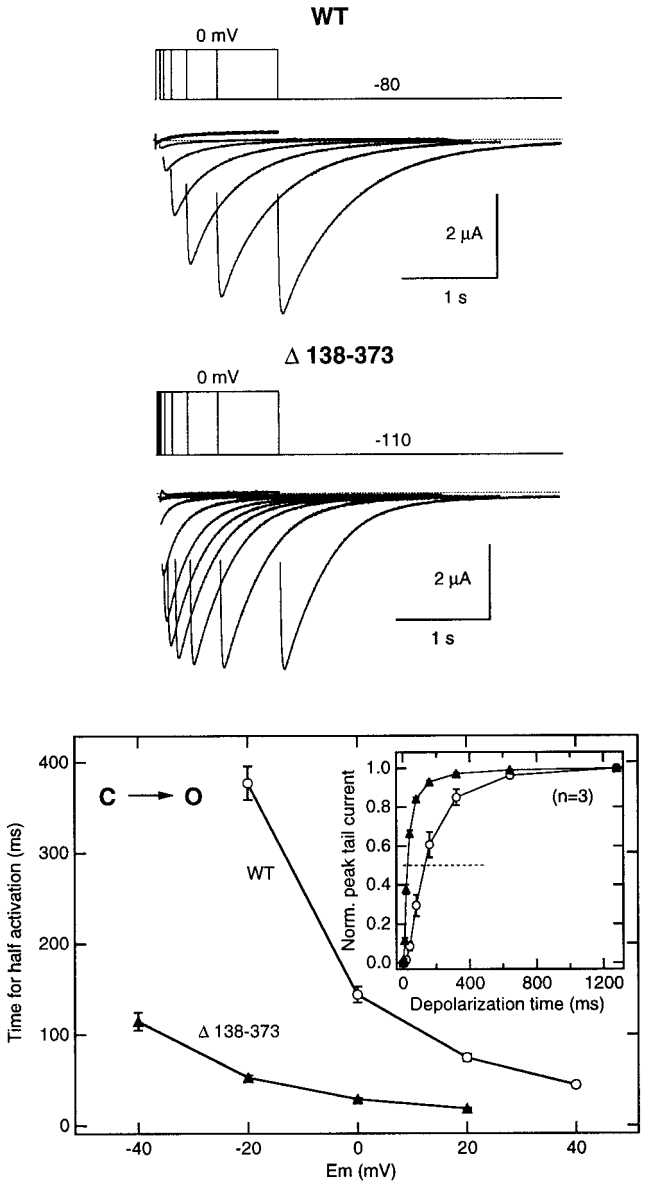

FIGURE 2 Effect of HERG proximal domain deletion on channel activation rates. (*Top*) The time course of voltage-dependent activation was studied by varying the duration of a depolarizing prepulse to 0 mV following the voltage protocols shown at the top of each current trace. Test pulses were applied once every 20 s. Families of currents from wild-type (WT) and proximal domain-deleted (Δ138–370) channels are shown. Note the −80-mV holding potential used for WT channels and the −110 mV used with the Δ138–373 construct. The zero current level is indicated by the dashed lines. (*Bottom*) Dependence of activation rates on depolarization membrane potential. The magnitude of the instantaneous tail currents upon repolarization was determined from recordings as shown at the top, by fitting exponentials to the decaying portion of the tail and extrapolating the current to the moment the depolarizing pulse was ended (Barros et al., 1998). Values correspond to 3–12 oocytes from three animals. Plots of normalized current values versus depolarization times were generated at the indicated voltages as shown in the inset for depolarizations to 0 mV, using three oocytes from the same frog. These plots were used to measure times necessary to attain half-maximum current magnitudes.

sitions during depolarization pulses by stepping the membrane to different voltages and measuring the initial magnitude of the tails after repolarizing the membrane (Fig. 3). Because of the slow rates of HERG activation and deactivation at voltages around the V_{half} values of the activation curves, very long pulses would be necessary to reach a complete steady state. This tends to reduce the viability of the clamped cells and, in some batches, to maximize the contribution of endogenous conductances to the recorded currents. Subsequently, we approached the steady state by established protocols (Schönherr et al., 1999). Thus depolarization pulses of up to 10 s duration were applied from two holding potentials: −80/−110 mV (for wild-type and proximal domain-deleted channels, respectively) to hold the channels fully closed and 0 mV to hold them fully open (Fig. 3 *A*). Subsequently, the position of the Boltzmann curves under true steady-state conditions (Fig. 3 *B, dashed lines*) was deduced from their coincidence at the longest depolarization times or as an extrapolated mean from the curves obtained at both holding potentials. This ensured that *I*/*V* curves were a function exclusively of test pulse characteristics, regardless of the previous (open or closed) state of the channels. Consistent with the measured resting potentials, the steady-state V_{half} activation values amounted to −59 mV and −80 mV in oocytes expressing wild-type and Δ138–373 HERG channels, respectively.

It is important to note that the observed modifications in activation parameters were not related to differences in holding potentials used with wild-type and deleted channels. Thus identical activation rates and activation voltage dependencies were obtained by holding wild-type channels between −80 and −120 mV or by maintaining the deleted channels at holding potentials ranging from −110 to −140 mV (not shown). This indicates that, at least in this range of potentials, HERG current characteristics are not affected by Cole-Moore effects, which otherwise would tend to increase the differences in activation between wild-type and mutant channels due to the maintenance of deleted variants at more negative holding potentials.

HERG deactivation time constants are not modified by deletion of the proximal domain

The strong modification in activation parameters induced by deletion of the HERG-specific domain strongly contrasts with the very similar deactivation properties exhibited by wild-type and deleted channels when they are driven to close once their opening is completed (Fig. 4 *A*; but see also below). Deactivation rates were obtained from the decaying portion of tail currents after depolarization pulses to fully open (and inactivate) the channels. Subsequently, the membrane was repolarized to different voltages, and after an initial phase of recovery from inactivation, the rate of tail current decay corresponding to channel closing was measured as indicated in Materials and Methods. As shown in

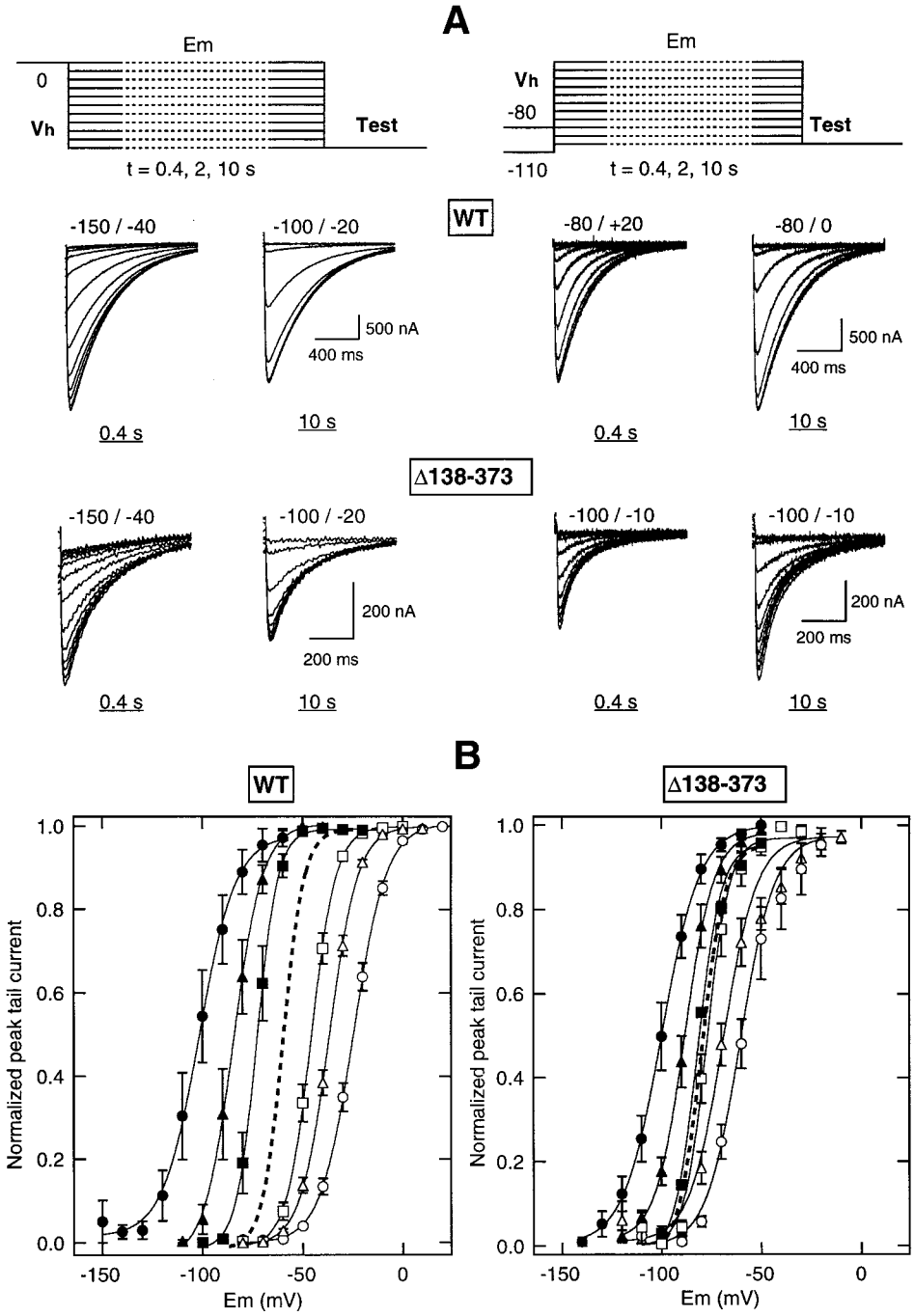

FIGURE 3 Effect of HERG proximal domain deletion on steady-state voltage dependence of activation. (*A*) Steady-state voltage dependence of activation was studied following the protocols shown in the two upper insets, with a prepulse of varying magnitude and a duration ranging from 0.4 to 10 s, followed by a pulse test to −100 mV. Holding potentials of 0 mV to hold the channels fully open (*left*) and −80 (WT) or −110 mV (Δ138–370) to hold the channels fully closed (*right*) were used as indicated. Families of tail currents during the test pulse for wild-type (WT) and proximal domain-deleted channels (Δ138–370) are shown. The range of potentials covered by the prepulse is stated at the top of each currents. The duration of the prepulse is shown underlined below the current traces. (*B*) Fractional activation curves for WT and Δ138–370 HERG channels. The closed and open symbols correspond to data obtained from zero and −80/−110 mV holding voltages, respectively. Data obtained at prepulse durations of 0.4 s (circles), 2 s (triangles), and 10 s (squares) are plotted. The continuous lines correspond to Boltzmann curves, $h(V) = I_{max}\ [1/(1 + \exp((V - V_{half})/k))]$, that best fitted the data. The dashed lines represent the deduced position of the activation curves under steady-state conditions obtained as a mean of those corresponding to both holding voltages and prepulses of 10-s duration. Values from at least four oocytes and two frogs are averaged in the graphs.

Fig. 4 *A*, HERG Δ138–373 deactivation time constants were indistinguishable from those of wild-type channels along the tested voltage range from −70 to −120 mV. Under these conditions, only an increase in the relative amplitude of the slowly deactivating component at negative voltages is consistently observed in the deleted channels (Fig. 4 *A*, *bottom right*). This demonstrates that whatever the alterations in channel gating induced by the deletion of the HERG-specific domain, they are mainly exerted in activation, not in deactivation parameters.

Effects of proximal domain removal are not related to HERG channel inactivation

A distinctive property of HERG is the presence of a rapid and voltage-dependent inactivation process that seems to constitute the mechanism for inward rectification (Smith et al., 1996). We studied the effects of proximal domain deletion on the onset of inactivation, using a dual-pulse protocol in which, after a depolarization to activate (and inactivate) the channels, the membrane is hyperpolarized briefly

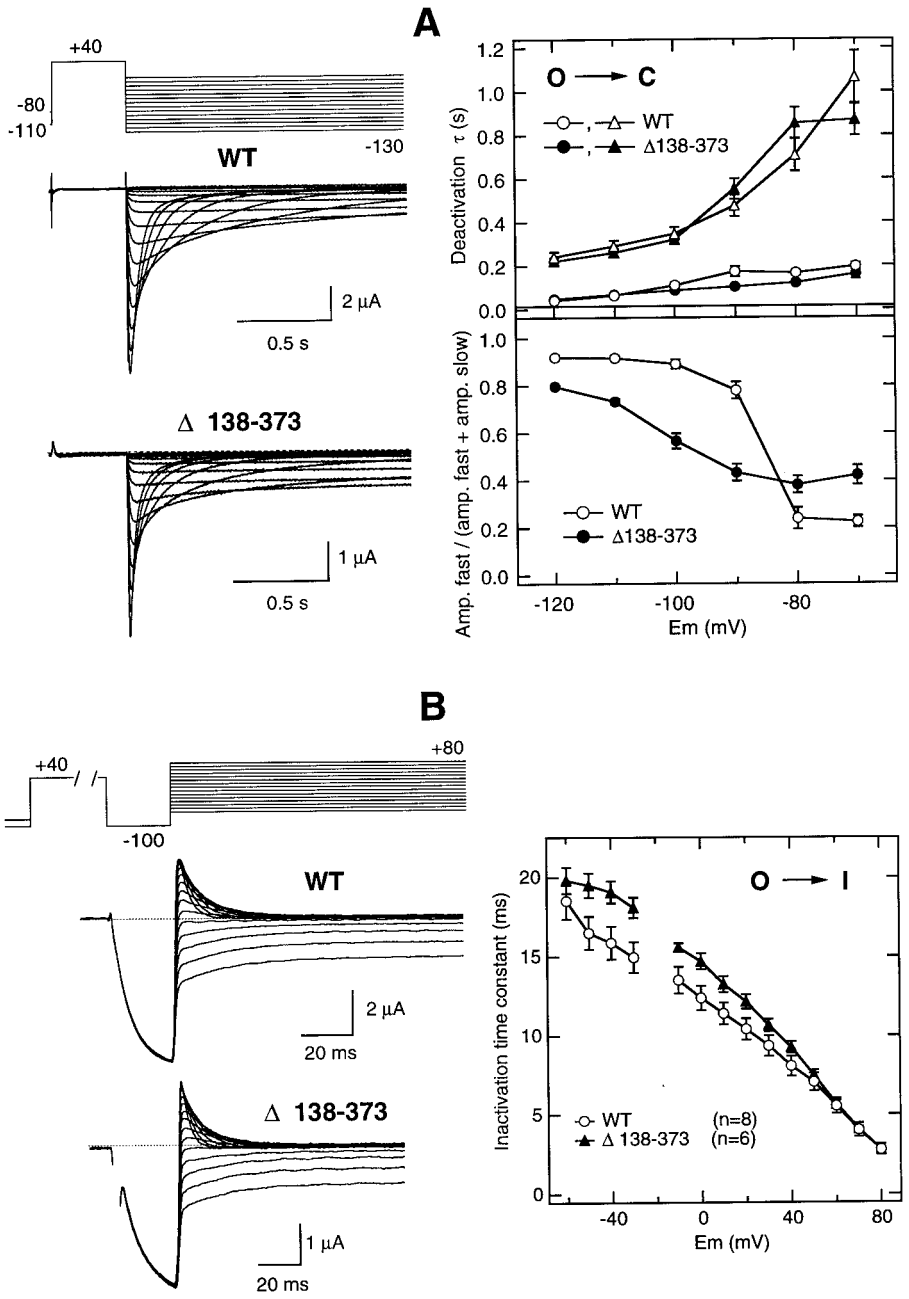

FIGURE 4 Lack of an effect of proximal domain deletion on HERG channel deactivation and inactivation rates. (*A*) Comparison of channel deactivation in wild-type and deleted channels. Families of currents from HERG wild-type (WT) and proximal domain-deleted channels (Δ138–373) are shown on the left. Currents were obtained during steps to potentials ranging from −130 to 0 mV, following depolarizing pulses to 0 mV, as indicated at the top of each trace. The zero current level is indicated by the dashed lines. Deactivation time constants were quantified by fitting a double exponential to the decaying portion of the tails as described in Materials and Methods. *Upper right panel*: Fast and slow deactivation time constants are plotted for different repolarization voltages. *Lower right panel*: The relative amplitudes of the fast components of deactivation for the two channel types. Averaged values are shown from nine oocytes expressing WT channels in which biexponential fits to the deactivation time course covering the full range of voltages could be performed for 26 cells ($N = 12$). Values from 23 oocytes ($N = 7$) were averaged for Δ138–373 channels. (*B*) Effect of proximal domain deletion on inactivation. Onset of fast inactivation was studied using the voltage protocol shown at the top. HERG was activated and inactivated with a 400-ms prepulse to +40 mV. A second short prepulse to −100 was used to recover the channels from inactivation, followed by a test pulse to different voltages to reinactivate the channels. Families of currents for wild-type (WT) and proximal domain-deleted channels (Δ138–373) are shown on the left. Test pulses were applied once every 20 s. Membrane currents are shown starting at the end of the depolarization prepulse. Time constants for the onset of inactivation as shown on the right were obtained from current traces by fitting a single-exponential function to the decaying portion of the currents during the test pulses. Holding potentials of −80 and −100 mV were used with WT and Δ138–373 channels, respectively. Note the small magnitude of the currents along the test pulses for voltages around the reversal potential of K^+ ions (≈ -20 mV). Statistical significance ($0.01 < p < 0.05$, Student's *t*-test) was obtained only for time constant values corresponding to voltages between +10 and −30 mV.

to allow them to enter the open state. A second depolarization pulse is then delivered to the cell, to follow the reinactivation of the channels (Smith et al., 1996; Barros et al., 1998). As shown in Fig. 4 *B*, the onset of inactivation follows a single-exponential rate from which the time constants for development of inactivation can be obtained. From these measurements it can be seen that inactivation becomes increasingly faster with increasing depolarization. However, the time constants of development of inactivation remained almost the same after deletion of the HERG-specific domain.

As a final demonstration that the elimination of the proximal domain almost exclusively modifies activation parameters of HERG, we obtained inactivation recovery rates for wild-type and deleted channels at different voltages from the rising hook of current records like those presented in Fig. 4 *A*. This measurement indicated that the inactivation recovery also remained unaltered after deletion of the proximal domain (data not shown).

The aforementioned results suggest that HERG-specific domain removal causes an effect on activation that is independent of inactivation transitions. To check the independence from inactive states, we measured changes in activation parameters, using channels lacking inactivation after replacement of Ser^{620} in the inner vestibule of the pore with threonine (S620T; see Suessbrich et al., 1997b; Ficker et al., 1998; Herzberg et al., 1998; Wang et al., 1998). As shown in Fig. 5, the activation properties of the channels remained almost unaffected by introduction of the methyl group at position 620 (compare with wild type in Fig. 2). Furthermore, an acceleration of activation rates (Fig. 5 *B*) and a shift in voltage dependence of activation (Fig. 5 *C*) equivalent to those induced by elimination of the proximal domain from wild-type channels were obtained with channels in which both the deletion and the inactivation-removing mutation were combined. Furthermore, similar closing rates were observed in wild-type, S620T, and S620T+Δ138–373 channels (not shown). This demonstrates that modification of activation parameters induced by removal of the HERG-specific domain is a direct effect that occurs even when the inactivation mechanism is disabled. That alterations in activation are equally manifested in S620T channels also validates the use of noninactivating channel variants carrying this mutation for easier performance of subsequent studies without contamination with inactivation processes.

Effects of proximal domain deletion are not related exclusively to its length, but also to elimination of specific amino acid sequences near the channel core

To determine whether the effect of HERG proximal domain deletion is similarly dependent on its length, we generated two channel variants in which nearly half of this domain was still preserved. The activation rates exhibited by channels lacking amino acids 223–373 (HERG Δ186–191 + 223–373 or Δ170–190 + 223–373; see Materials and Methods) were quite similar to those of the construct from which the whole HERG-specific domain was deleted (data not shown). In an attempt to further delimit the specific region(s) involved in the regulation of activation properties, we also generated and characterized a construct carrying a short 19-amino acid deletion near the core of the channel protein (HERG Δ355–373; Fig. 1). The activation rates of the Δ355–373 variant lay between those of wild-type and fully proximal domain-deleted channels. Furthermore, deactivation rates analogous to those of full-length HERG were observed with all of these constructs partially deleted in the proximal domain (not shown).

For a more direct detection and quantification of gating alterations, because they are independent of channel inactivation (see above), we also studied the effect of partial deletions in S620T mutant channels lacking inactivation. In this case, the time needed to attain half-activation was obtained directly from the current traces along depolarization pulses to different potentials. As shown in Fig. 6, *A* and *B*, quite similar activation rates were obtained with channels lacking the whole proximal domain (S620T+Δ138–373) and those in which nearly half of this domain was preserved (S620T+Δ223–373). Furthermore, around half of the acceleration of activation induced by removal of the whole proximal domain was still present in S620T+Δ355–373 channels, despite the fact that only 19 residues (corresponding to less than 10% of the total proximal domain length) have been removed in this construct. Again, deactivation time constants like those of wild-type channels were obtained with these variants when they were driven to close from fully activated states following long pulses to positive voltages (data not shown, but see also below). Thus, as illustrated more quantitatively in Fig. 6 *B* for measurements performed at 0 mV, an increasingly slower opening is induced by an increasing number of amino acids in the proximal domain; this trend is particularly significant in the presence of residues located between positions 355 and 373 of the HERG sequence.

As a further indication of the relevance of different regions of the proximal domain regulating HERG properties, the activation voltage dependencies of channels with different deletions were compared in the background of both wild-type and noninactivating channels. As shown in Fig. 6 *C* for noninactivating variants, the positions of the steady-state activation curves along the voltage axis are quite similar for Δ138–373 and Δ223–373 deleted channels. Furthermore, nearly half of the hyperpolarizing shift caused by these deletions is still obtained with the expression of Δ355–373 HERG. Almost identical results were obtained by using normally inactivating channels with a serine in position 620 but carrying the same deletions (data not shown).

That elimination of only 19 amino acids is able to induce nearly half of the effect caused by removal of either 157 (Δ186–191 + 223–373) or 236 (Δ138–373) residues supports the conclusion that the effects of HERG-specific do-

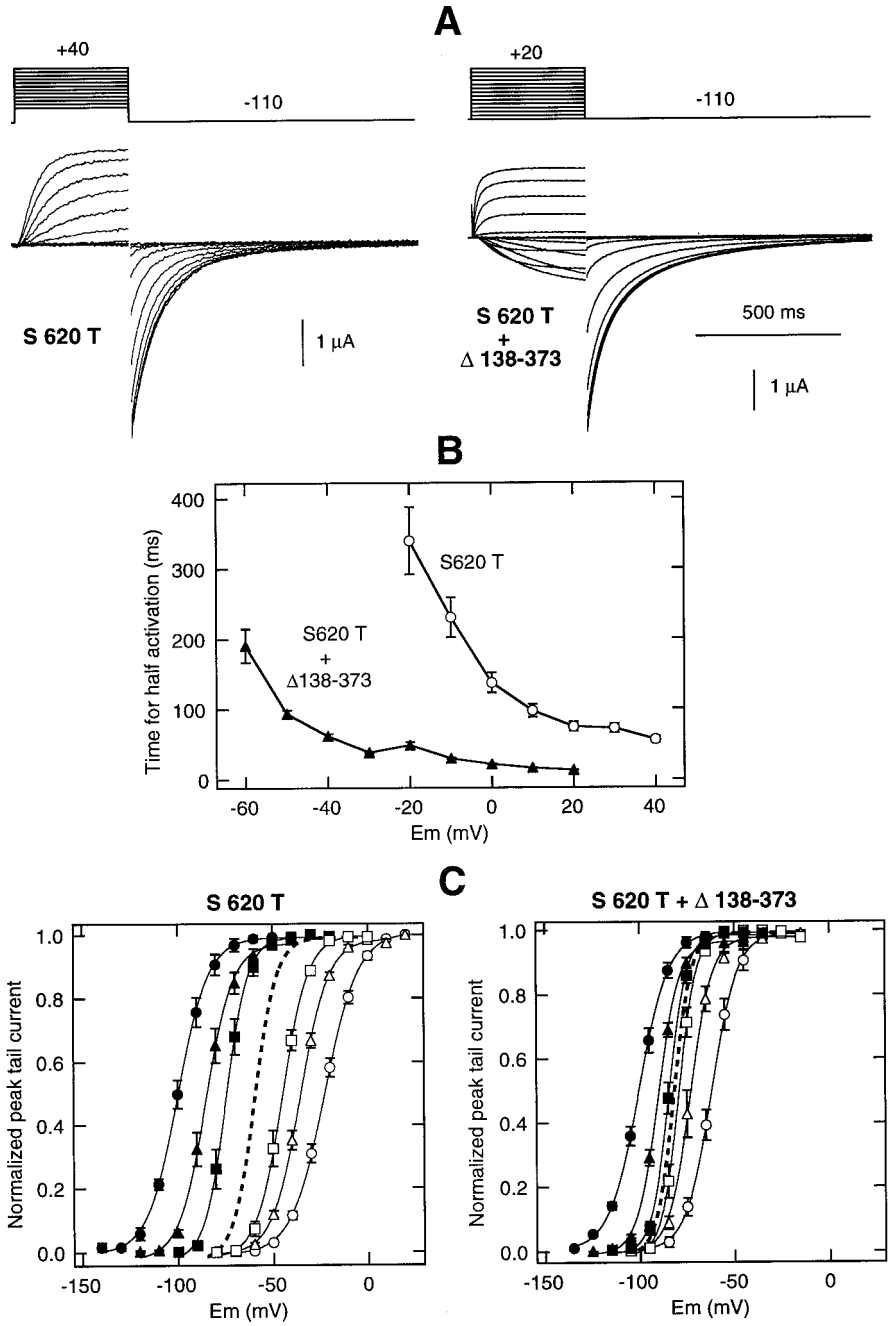

FIGURE 5 Effects of proximal domain removal are independent of HERG inactivation. (*A*) Families of currents with 400-ms steps to different voltages applied to channels carrying a point mutation to abolish channel inactivation, combined (S620T+Δ138–373) or not combined (S620T) with a deletion removing the proximal domain from the amino terminus. Note the faster activation time course of proximal domain-deleted channels at every depolarization voltage. (*B*) Dependence of activation rates on membrane potential. Times for half-activation were obtained directly from current traces as in *A* measuring the time necessary to attain half of the maximum current at every depolarization voltage. Averaged values from seven and 10 oocytes ($N = 3$) are shown for full-length and proximal domain-deleted channels, respectively. (*C*) Steady-state voltage dependence of activation for S620T and S620T+Δ138–373 channels. The magnitude of the tail currents during test pulses and the Boltzmann fits to the data were obtained as indicated in the legend of Fig. 3.

main deletion are not related exclusively to the length of this domain. Furthermore, this suggests that the short stretch of amino acids between residues 355 and 373 is important in determining the role of the proximal domain for the regulation of HERG activation properties. Whether this is due to a direct interaction of this particular sequence with the gating machinery or to an indirect effect via the *eag* or other protein domain(s) remains to be established. Finally, our results indicate that some residue(s) between positions 223 and 355 of the proximal domain can also help to maintain the slow activation rates and the positive voltage dependence of activation exhibited by full-length HERG channels.

Possible interactions between distal *eag* and HERG-specific proximal domains in the amino terminus

Modifications in HERG activation induced by removal of the proximal domain are reverted by additional deletion of the eag domain

Previous studies with HERG deletion mutants lacking the whole amino terminus indicated a huge acceleration of deactivation kinetics, leading to the proposal that the amino-terminal portion of HERG is involved in channel gating but does not mediate channel inactivation (Schönherr and Hei-

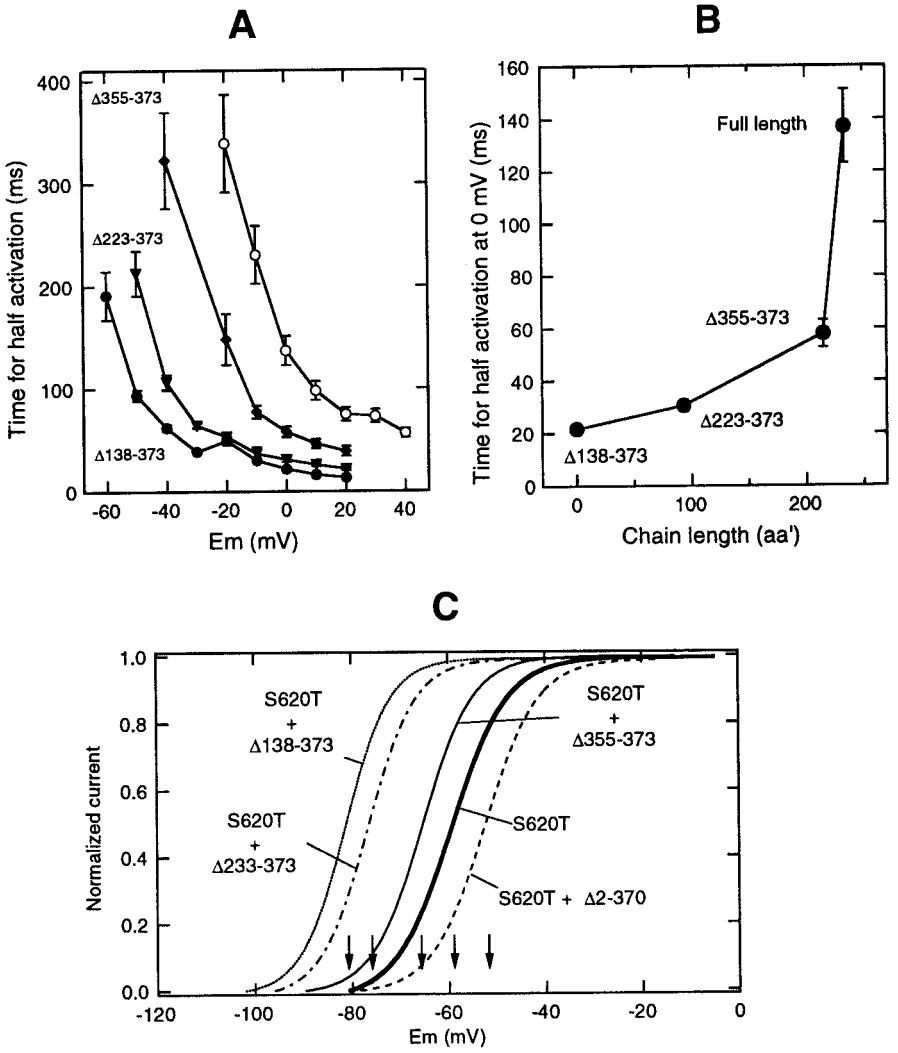

FIGURE 6 Influence of proximal domain length in HERG activation. (*A*) Dependence of activation rates on membrane potential in channels carrying different deletions of the proximal domain. Times for half-activation were obtained directly from current traces, using noninactivating S620T channels and measuring the time necessary to attain half of the maximum current at every depolarization voltage. Values from wild-type (WT) and whole proximal domain-deleted channels (Δ138–373) like those in Fig. 5 are shown for comparison. (*B*) Time for half-activation at 0 mV as a function of proximal domain length. The channel variants are arranged in the abscissa in increasing length of the proximal domain, corresponding to Δ138–373, Δ186–191 + 223–373 (Δ223–373 on the graph; see Materials and Methods), Δ355–373, and full-length channels. (*C*) Steady-state activation voltage dependence of wild-type and amino-terminus-deleted HERG channels. The voltage dependencies of activation under steady-state conditions were derived following the procedures detailed in the legend of Fig. 3. Different HERG channel variants carrying the indicated deletions in the amino terminus were used after being introduced into the background of the S620T noninactivating HERG. The relative positions of the V_{half} values of the Boltzmann curves along the voltage axis are indicated by arrows.

nemann, 1996; Spector et al., 1996b). Knowing the profound impact of selective removal of the HERG-specific domain on HERG activation (see above), we characterized the activation kinetics by using a channel variant in which both the *eag* and the proximal domains had been deleted (Δ2–370; Fig. 1). Surprisingly, the activation voltage dependence of the Δ2–370 constructs appeared to be shifted slightly to positive values as compared to those of full-length channels (Fig. 6 *C*). Furthermore, the activation of the Δ2–370 variant was not as strongly accelerated as in Δ138–373 channels lacking only the proximal domain. Thus only a modest enhancement of activation rates was obtained upon expression of the Δ2–370 construct (Fig. 7), yielding activation kinetics superimposable on those of channels lacking the 19 amino acids between residues 355 and 373. These results were obtained when the Δ2–370 deletion was introduced in normal HERG or in noninactivating S620T channels. Furthermore, as repeatedly reported by others (Schönherr and Heinemann, 1996; Spector et al., 1996b; Wang et al., 1998; Cabral et al., 1998), closing rates accelerated by around an order of magnitude were obtained at negative voltages in Δ2–370 channels lacking most of the amino terminus (not shown).

This demonstrates that the modifications in activation parameters induced by removal of the HERG-specific domain are compensated for, at least partially, by additional elimination of the *eag* domain. It also suggests that the presence of an intact *eag* domain, perhaps interacting with the gating machinery, could constitute an important factor that not only slows channel deactivation, but also participates in the alterations in activation induced by deletion of the proximal domain.

Deletion of the proximal domain accelerates transition of HERG to state(s) showing slow deactivation rates

The results presented above suggest that in addition to its known effect of slowing down HERG closing (Wang et al.,

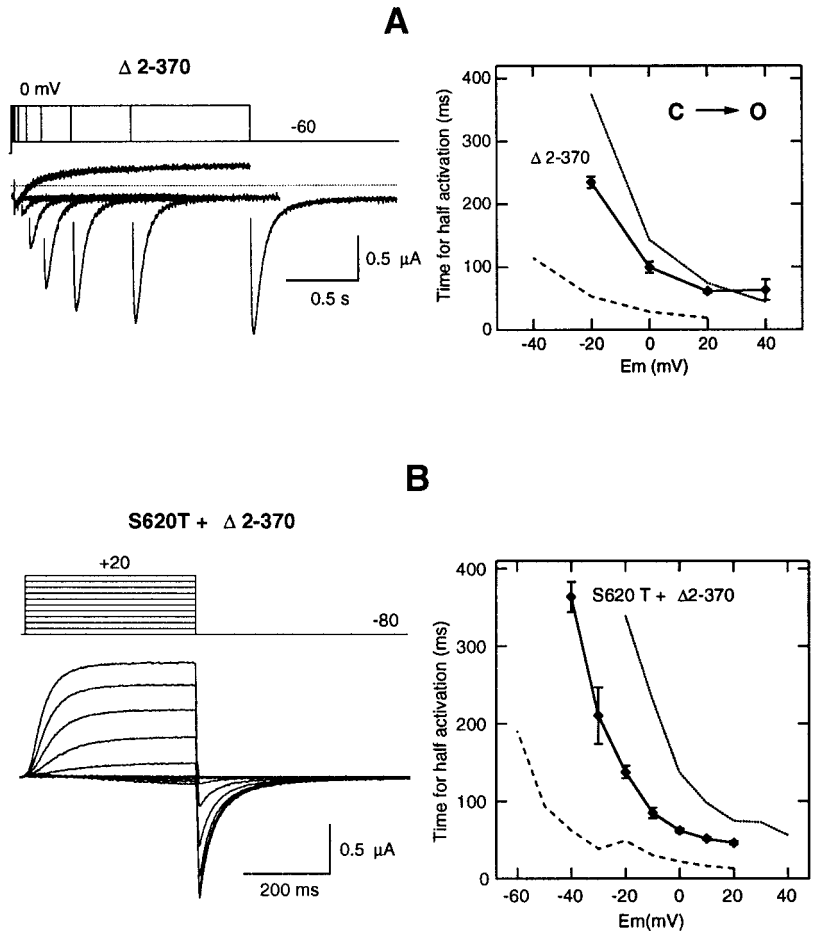

FIGURE 7 Proximal domain deletion-induced accelerations in activation are partially compensated for by the additional removal of the *eag* domain. *(A)* Activation rates of HERG Δ2–370 channels. A family of currents obtained by varying the duration of a depolarizing pulse to 0 mV is shown on the left. Repolarization steps to −60 mV to slow down channel deactivation and allow proper measurements of tail current magnitudes were delivered as shown. The dependence of activation rates on depolarization potential is shown on the right. The magnitude of the instantaneous tail currents upon repolarization was determined from recordings as shown on the left, by fitting an exponential to the decaying portion of the tail and extrapolating the current to the moment the depolarizing pulse was ended. (*B*) Activation rates of S620T noninactivating HERG channels carrying a Δ2–370 deletion. A family of currents in response to 400-ms depolarizations to different voltages is shown on the left. Times for half-activation were obtained directly from current traces measuring the time necessary to attain half of the maximum current at every depolarization voltage. Lines showing the variation of activation rates as a function of voltage for wild-type (·····) and Δ138–373 channels (– – –) are also shown for comparison.

1998; Cabral et al., 1998; Sanguinetti and Xu, 1999), the interaction of the *eag* domain with the channel leads to an acceleration of activation in the proximal domain-deleted variant. However, such acceleration is only manifested if the proximal domain is removed, because constructs lacking the *eag* domain show an activation behavior reminiscent of that exhibited by full-length channels. To test the possibility that the presence of the long proximal domain characteristic of HERG is able to constrain the interaction of the *eag* domain with the channel protein, limiting or delaying its influence up to the moment at which channel activation has been substantially advanced, we compared the rates at which both wild-type and proximal domain-deleted channels close at a constant repolarization potential, as a function of the depolarization voltage or the depolarization time used to activate them. To prevent any influence of inactivation and/or inactivation recovery steps in the results, we conducted experiments with S620T channels from which inactivation had been removed.

As shown in Fig. 8, *A* and *B*, slow closing rates were observed with proximal domain-deleted channels that remained unaltered along the whole range of voltages at which current activation took place. However, although slow deactivation rates analogous to those of deleted channels were observed in wild-type channels at positive voltages (see also Fig. 4 above), significantly faster deactivation rates were measured in response to depolarizations at which full activation is not reached. Interestingly, the voltage dependence of the increase in deactivation time constant appeared to be superimposable on the activation voltage dependence of full-length but not of proximal domain-deleted channels (Fig. 8 *B*). This suggests that full-length channels, the activation of which is not influenced early by the *eag* domain because of the restricting influence of the proximal domain, close fast until full activation has been achieved at long times or very positive voltages. In contrast, proximal domain-deleted channels would close slowly along their activation voltage range because of the presence of the *eag* domain interacting with the channel, as indicated by the faster activation rates and left-shifted activation voltage dependencies. Whether this is due to a permanent *eag* domain-channel interaction or to a very fast association of this domain that precedes the transition to the open state remains to be established. Nevertheless, assuming a three-closed-state model, as recently proposed for HERG opening

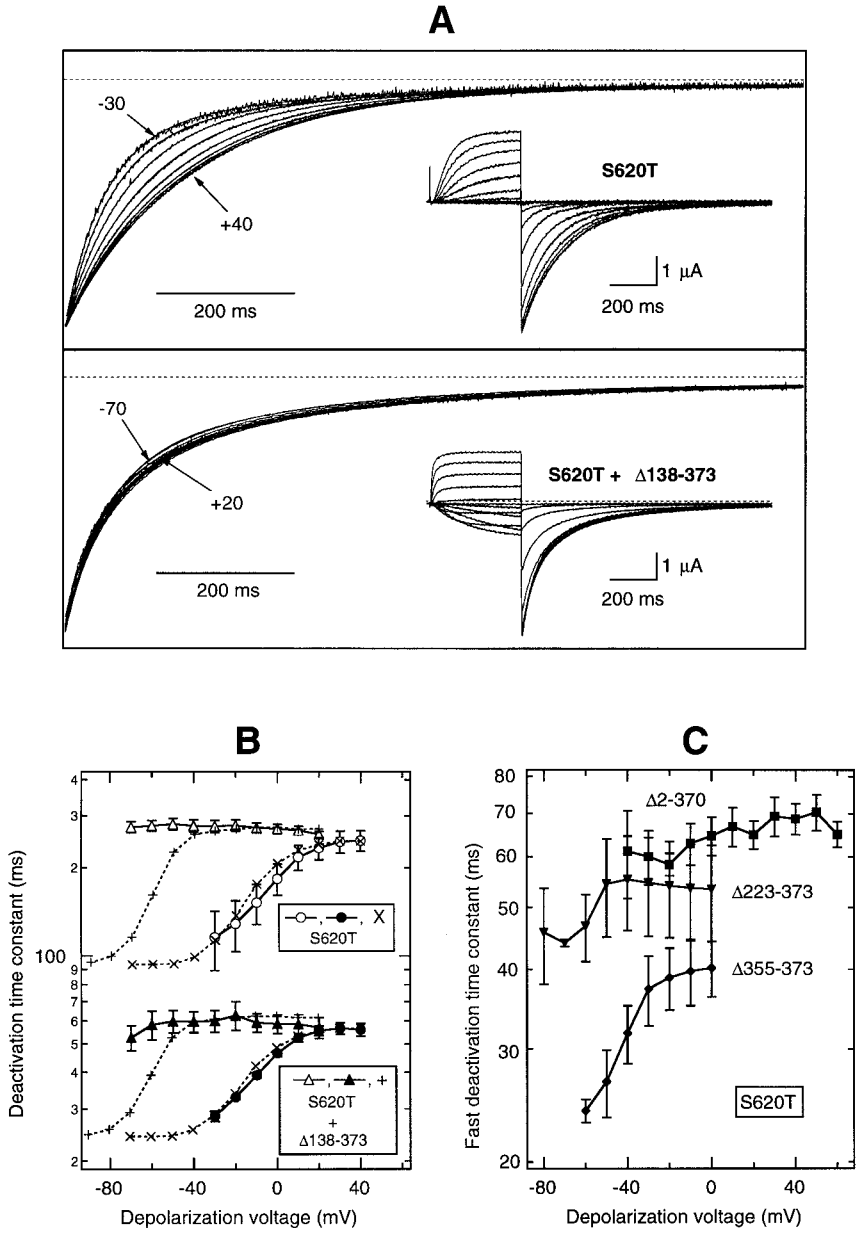

FIGURE 8 Proximal domain removal accelerates transitions to slowly deactivating HERG channel state(s). (*A*) Scaled deactivating tail currents in response to depolarization steps to different potentials. Noninactivating full-length (S620T) or proximal domain-deleted (S620T+Δ138–373) channels were submitted to 400-ms depolarization pulses to different voltages between −70 and +40 mV (S620T) or −90 and +20 mV (S620T+Δ138–373) in 10-mV steps from a holding potential of −110 mV. Note the slower rates of deactivation induced by increasing depolarization voltage in full-length but not in proximal domain-deleted channels. Biexponential fits are also shown superimposed on the tails. Currents induced by depolarizations and tail currents after repolarization to −110 mV are shown in the insets. (*B*) Variation of HERG deactivation rates as a function of depolarization voltage. Time constants for deactivation were obtained as indicated in Materials and Methods from tail current recordings as in *A*. The percentage of the fast decaying tail current component oscillated between 80% at −30 mV and 95% at +40 mV for S620T channels. It also remained fairly constant around 60–70% in the range of −70 to +20 mV for S620T+Δ138–373 channels. Averaged values from six oocytes from the same batch are shown. *I/V* curves for the tail currents of the insets in *A* are also shown against an arbitrary vertical scale for better comparison of the voltage dependence of activation and deactivation slowing in S620T (×) and S620T+Δ138–373 (+) channels under the same conditions. (*C*) Variation of HERG deactivation rate as a function of depolarization voltage in channels carrying different deletions in the amino terminus. Time constants of deactivation were obtained as detailed in the legend of Fig. 8 from tail current recordings of oocytes expressing S620T noninactivating channels, from which nearly half of the proximal domain (Δ223–373), 19 residues (Δ355–373), or both the *eag* and the proximal domains (Δ2–370) had been deleted. Averaged values from four oocytes are plotted against the amplitude of the depolarization step. Only values corresponding to the major fast component of deactivation are plotted, for simplicity. Repolarization voltage for recording tail currents was −110 mV for Δ223–373 and Δ355–373 constructs. Repolarization steps to −60 mV were used with Δ2–370 channels to slow down channel deactivation and allow proper measurement of deactivation time constants. Nevertheless, although with faster closing kinetics, similar results were obtained with repolarization to −110 mV.

(S. Wang et al., 1997; Kiehn et al., 1999),

$$C_0 \rightarrow C_1 \rightarrow C_2 \rightarrow O$$

Scheme I

our data indicate that removal of the proximal domain accelerates transitions through closed states. Thus the sigmoid delay in activation kinetics (an indication of the C_0 to C_1 transition rate; S. Wang et al., 1997) was clearly reduced in Δ138–373 channels, even when the left shift in activation voltage dependence caused by the deletion is taken into account (e.g., compare onset of the current traces upon depolarization to +40 and 0 mV for S620T and S620T+Δ138–373, respectively, in Fig. 8 *A, insets*). Furthermore, when the saturation of the late time constants of activation at positive potentials (an indication of the limitation in activation kinetics imposed by the voltage-independent step from C_1 to C_2; see S. Wang et al., 1997) was studied in the currents shown in the insets of Fig. 8 *A*, asymptotic values of 52 and 21 ms were obtained for the forward rate constant of the C_1-to-C_2 transition in full-length and proximal domain-deleted channels, respectively.

When the influence of depolarization voltage in the closing rates was characterized in channels carrying other deletions in the amino terminus, the results shown in Fig. 8 *C* were obtained. It is observed that the fast rates of deactivation (accounting for most of the tail current magnitude) in Δ223–373 channels lacking nearly half of the HERG-specific domain remained almost the same along the range of voltages at which activation took place. This would be consistent with the quite similar behavior of these channels and those in which the whole proximal domain was deleted. As expected from the absence of the *eag* domain, the deactivation kinetics of Δ2–370 channels were not affected by depolarization voltage. Furthermore, a slowing-down of closing with increasing depolarization was obtained in channels lacking the 19 residues between positions 355 and 373. However, this effect was manifested at voltages more negative than those at which it happened in full-length channels.

As an additional support for our conclusions, we also studied the effect of increasing depolarization time on closing kinetics (Fig. 9). In this case, the cells were depolarized to voltages yielding similar activation rates for full-length and deleted channels (Fig. 9 *A*). For full-length channels, the deactivation rates with short depolarizations appeared significantly faster than those obtained after longer depolarization steps (Fig. 9, *A–C*). These differences were particularly prominent when we looked at the fast deactivating component of the tails, which otherwise accounted for most of the current amplitude at the repolarization potential used (Fig. 9 *D*). In contrast, similar and slow deactivation rates were obtained in Δ138–373 deleted channels after depolarization steps in the whole range of duration (20–300 ms) at which appreciable tail currents could be recorded. Again, the time course of deactivation time constant increases runs parallel to the increase in the fraction of channel opening for the full-length variant. However, only a quite constant and slow deactivation rate was exhibited by Δ138–373 channels, even at short depolarization times at which small current activations have been induced (compare data in Fig. 9, *A* and *C*).

In summary, because slowed closing is a good indication of *eag* domain-channel interaction (Wang et al., 1998; Cabral et al., 1998; Sanguinetti and Xu, 1999), our results indicate that the opening of the proximal domain-deleted channels is taking place in the presence of an *eag* domain-channel interaction, but that the activation of the full-length channels is completed before such an interaction takes place, because of the restricting influence of the proximal domain. Furthermore, they suggest that in the deleted variant a cause-effect relationship exists between the interaction of the *eag* domain with the channel protein and modification of the activation properties.

DISCUSSION

One characteristic structural feature of HERG K^+ channels as compared to other members of the *eag* family, is the presence of a long stretch of amino acids (designated here as the HERG-specific or proximal domain) that separates the conserved initial *eag* or PAS domain from the core of the channel protein (see above). Previous studies with deletion mutants in which either the *eag* or both the *eag* and the HERG-specific domains were removed indicated that the amino terminus of HERG does not participate in the fast inactivation process, but contributes to control channel deactivation (Schönherr and Heinemann, 1996; Spector et al., 1996b; Wang et al., 1998; Cabral et al., 1998). By selectively removing the long HERG-specific domain, we demonstrate here a strong acceleration of channel opening. This is associated with a shift of activation voltage dependence in the hyperpolarizing direction. However, elimination of the HERG-specific domain has almost no effect on the closing and inactivation properties of the channel. Thus two different domains regulating HERG gating seem to exist in the amino terminus: a distal *eag* domain mainly controlling current deactivation, and a HERG-specific domain regulating current activation. Removal of the *eag* domain from the deleted channels noticeably reverses the effects on activation caused by selective elimination of the proximal domain. This indicates that the functional consequences of proximal domain removal for channel opening are at least partially dependent on the presence of the *eag* domain and suggests that an interaction of the *eag* domain with the channel core is involved in modifications of activation caused by elimination of the HERG-specific domain.

These results are compatible with a model in which the presence of the long domain exclusive of HERG limits or

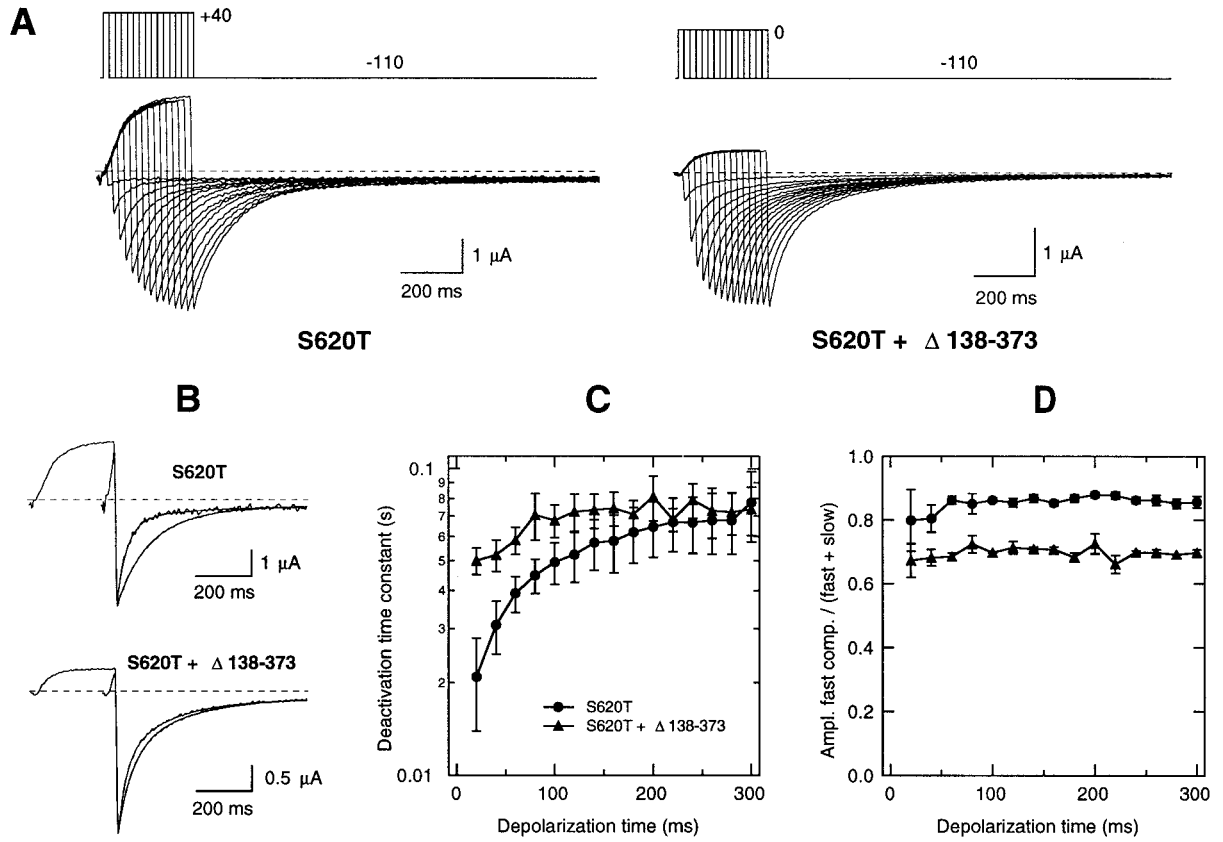

FIGURE 9 Effect of depolarization time on closing rates of full-length and proximal domain-deleted HERG channels. (*A*) Currents induced by depolarizations of different duration in oocytes expressing full-length (S620T) and proximal domain-deleted (S620T+Δ138–373) noninactivating HERG channels. (*B*) Scaled currents in response to depolarization steps of 40 and 300 ms. Current traces are shown displaced along the horizontal axis for coincidence of the tail current time course. Tail current magnitude has been normalized to peak. Biexponential fits are also shown superimposed on the tail currents. (*C*) Variation of HERG deactivation rates as a function of depolarization time. Fast and slow deactivation time constants were obtained from tail current recordings of four oocytes ($N = 2$) as in *A*. Only values corresponding to the major fast component of deactivation are plotted. (*D*) Relative amplitude of the fast deactivation component in full-length and proximal domain-deleted channels with depolarizations of increasing duration, as indicated on the abscissa.

slows down the interaction of the *eag* domain with the channel core. Elimination of the proximal domain would favor the interaction of the *eag* domain with the gating machinery, speeding up activation. Furthermore, it could be also expected that once activation has been completed at longer times or more positive voltages in full-length channels, dissociation of the *eag* domain from its interaction site(s) limits deactivation, making this process scarcely dependent on the presence of the proximal domain. In this case, the requirement of channel opening for effective interaction of the *eag* domain with the channel is supported by the coincidence of the time course and voltage dependence for channel activation and slowing of deactivation, a characteristic dependent upon the presence of an *eag* domain interacting with the channel core (Wang et al., 1998; Cabral et al., 1998; Sanguinetti and Xu, 1999). Further support for this model comes from the behavior of constructions in which the whole amino terminus has been deleted. In this case, the facilitating contribution of the *eag* domain to opening will be removed, yielding activation properties more similar to those of the wild-type channel, which has this domain separated from the protein core by the proximal domain. Furthermore, *eag* domain removal would also remove the limitation imposed by its relatively slow dissociation. This would explain the marked acceleration of closing rates observed with variants lacking either the whole amino terminus or the initial residues of the HERG protein (London et al., 1997; Cabral et al., 1998; Wang et al., 1998). Finally, albeit indirectly, the proposed model is also supported by our recent observation that in full-length channels a temperature increase from 24°C to 35°C causes a nearly fourfold decrease in the time needed for half-activation, but a less than twofold decrease in deactivation time constants (Barros and Pardo, manuscript in preparation). Thus more extensive conformational changes seem to be required for channel opening as compared to deactivation, a process probably rate-limited by unbinding and diffusion of the *eag* domain.

Opening of HERG channels has been described recently as a multistep sequential process in which the final and voltage-dependent closed-to-open transition is preceded by two steps between closed states: an initial one that is weakly voltage dependent, and a second that is essentially voltage independent (S. Wang et al., 1997; Wang et al., 1998; Kiehn et al., 1999; see also above). Our data indicate that both transitions are clearly accelerated in proximal domain-deleted channels and that the time constant of the slowest voltage-independent transition (S. Wang et al., 1997) is reduced by more than half by the deletion. Although the structural rearrangements associated with individual transitions are not known, this suggests that the need to adequately modify the conformation of the exclusive HERG proximal domain acts as an important constraining factor on efficient progress through the activation pathway.

The exact identity and position of the regulatory residues in the proximal domain are not known, but our results demonstrate that some of them are located between amino acids 223 and 373, close to the core of the channel protein. Our results indicate that a short stretch of 19 amino acids between residues 355 and 373 is important in limiting the interaction of the *eag* domain with the channel core. However, other residues located between positions 223 and 355 may also help to prevent the effect of this domain favoring activation. Interestingly, removal of residues 355–373 eliminates five positive charges from the HERG sequence. Thus it is tempting to speculate on the possibility that the presence of this region exerts an electrostatic repulsion of the otherwise positively charged distal amino terminus. Systematic mutagenesis studies directed at locating the specific residue(s) involved in proximal domain deletion effects are currently under way.

Previous work with *Shaker* channels in which the length of the amino-terminal chain domain was systematically changed indicated that ball-dependent channel inactivation was accelerated by chain deletions and slowed by amino acid insertions (Hoshi et al., 1990). As for the interaction of the ball with N-type inactivating channels, the coincidence of voltage dependence for HERG activation and slowing of deactivation suggests that the interaction of the *eag* domain with HERG is intrinsically voltage independent, and any apparent voltage dependence would arise from direct coupling to activation. Furthermore, the S4-S5 linker seems to act as a receptor site for the very amino terminus in both N-type-inactivating *Shaker* (Holmgren et al., 1996) and HERG channels (Cabral et al., 1998; Wang et al., 1998; Sanguinetti and Xu, 1999). Thus it could be possible that a mechanism similar to that of N-type inactivation is operative in HERG. However, the concept of "ball" and "chain" domains applied in the framework of a diffusible blocking particle that interacts with the channel core with kinetics dependent on the length of a flexible chain domain (Hoshi et al., 1990) does not seem to be directly applicable to HERG. Thus 1) activation/deactivation gating and not inactivation properties is regulated by the HERG amino terminus; 2) the influence of the proximal domain in HERG gating is exerted through the presence of specific sequence patterns and is not exclusively related to chain length; 3) there is no indication that the amino terminus blocks the HERG pore (Wang et al., 1998); 4) although amino-terminus action is disrupted by elevating external K^+ in both *Shaker* (Demo and Yellen, 1991) and HERG (Wang et al., 1998) channels, higher concentrations seem to be needed to destabilize the interaction of the HERG amino terminus with the channel core; 5) only a single ball domain is required to mediate N-type inactivation, but more than one and possibly all four amino termini could be involved in HERG deactivation slowing (Wang et al., 1998); and 6) unlike the case of the ball-inactivating particle, it has been proposed that the distal *eag* domain is tightly attached to the body of the channel protein (Cabral et al., 1998). It is important to note also that in addition to amino-terminal domains, other cytoplasmic structures could also be involved in the regulatory effects on HERG gating. Thus shifts in activation voltage dependence, such as those induced by removal of the HERG proximal domain, are produced when the HERG carboxy terminus is replaced by the equivalent domain of mouse *eag* (Herzberg et al., 1998). Similarly, both amino and carboxy termini modulate the voltage sensitivity of KAT1 channels (Marten and Hoshi, 1998).

The regulatory effects of rat *eag* and KAT1 amino-terminal domains on activation voltage dependence and kinetics seem to be exerted through their molecular interaction with the S4 segment or the S4-S5 linker (Terlau et al., 1997; Marten and Hoshi, 1998). Residues in the S4-S5 linker of *Shaker* also act as receptor sites for the distal inactivation ball and influence activation gating (Holmgren et al., 1996). Similarly, the interaction site(s) of the very amino terminus with HERG channels seems to be located in the S4-S5 loop (Cabral et al., 1998; Wang et al., 1998; Sanguinetti and Xu, 1999). Whether the modulatory effects of the HERG proximal domain are indirect or are exerted by a direct interaction of this domain with the distal *eag* domain or with the gating machinery remains to be established.

Regardless of the molecular mechanism(s) involved in controlling gating behavior, the combination of an *eag* domain with the HERG-specific proximal domain seems to explain two important features of the channel that help it to achieve its physiological role. One is the slow activation rate, essential for use-dependent accumulations implicated in the spike-frequency accommodation of neuronal firing (Schönherr et al. 1999) and, in combination with the very fast inactivation characteristic of HERG, for limiting the outward flow of K^+ ions and contributing to the maintenance of the plateau potential in cardiac cells (Hancox et al., 1998). This is needed to limit the interaction of the *eag* domain with the channel core, and hence this would not be achieved without the proximal domain. The other feature is

the slow deactivation rate upon repolarization as compared to that obtained without the *eag* domain. In addition to the small depolarization-induced currents due to superposition of slow activation and fast inactivation, this *eag* domain-dependent effect would ensure the known operation of HERG as an inward rectifier. This would also determine the important participation of HERG not only in the repolarization phase of the cardiac action potential (and subsequently in controlling the duration of the spike and interspike intervals; Smith et al., 1996, Zhou et al., 1998), but also in the maintenance of the resting potential, the electrical excitability, and the pacemaking activity of adenohypophysial, neuronal, cardiac, and tumor cells (Barros et al., 1997; Bianchi et al., 1998; Schäfer et al., 1999; Schönherr et al., 1999).

We thank Dr. Enzo Wanke for kindly providing the HERG channel-containing plasmid.

CGV holds a predoctoral fellowship from the Dirección General de Investigación Científica y Técnica (DGICYT) of Spain. TG is a predoctoral fellow from the University of Oviedo. DG-V is supported by the Fundación Inocente, Madrid, Spain. This work was supported by grant PB96-0316 from the DGICYT of Spain.

REFERENCES

Arcangeli, A., A. Becchetti, A. Mannini, G. Mugnai, P. De Filipi, G. Tarone, M. R. Del Bene, E. Barletta, E. Wanke, and M. Olivotto. 1993. Integrin-mediated neurite outgrowth in neuroblastoma cells depends on the activation of potassium channels. *J. Cell. Biol.* 12:1131–1143.

Arcangeli, A., L. Bianchi, A. Becchetti, L. Faravelli, M. Coronnello, E. Mini, M. Olivotto, and E. Wanke. 1995. A novel inward-rectifying K^+ current with a cell-cycle dependence governs the resting potential of mammalian neuroblastoma cells. *J. Physiol. (Lond.).* 489:455–471.

Barros, F., D. del Camino, L. A. Pardo, T. Palomero, T. Giráldez, and P. de la Peña. 1997. Demonstration of an inwardly rectifying K^+ current component modulated by thyrotropin-releasing hormone and caffeine in GH3 rat anterior pituitary cells. *Pflügers Arch.* 435:119–129.

Barros, F., D. Gómez-Varela, C. G. Viloria, T. Palomero, T. Giráldez, and P. de la Peña. 1998. Modulation of human erg K^+ channel gating by activation of a G protein-coupled receptor and protein kinase C. *J. Physiol. (Lond.).* 511:333–346.

Barros, F., C. Villalobos, J. García-Sancho, D. del Camino, and P. de la Peña. 1994. The role of the inwardly rectifying K^+ current in resting potential and thyrotropin-releasing hormone-induced changes in cell excitability of GH3 rat anterior pituitary cells. *Pflügers Arch.* 426: 221–230.

Bianchi, L., B. Wible, A. Arcangeli, M. Taglialatela, F. Morra, P. Castaldo, O. Crociani, B. Rosati, L. Faravelli, M. Olivotto, and E. Wanke. 1998. *herg* encodes a K^+ current highly conserved in tumors of different histogenesis: a selective advantage for cancer cells? *Cancer Res.* 58: 815–822.

Bixby, K. A., M. H. Nanao, N. V. Shen, A. Kreusch, H. Bellamy, P. J. Pfaffinger, and S. Choe. 1999. Zn^{2+}-binding and molecular determinants of tetramerization in voltage-gated K^+ channels. *Nature Struct. Biol.* 6:38–43.

Cabral, J. H. M., A. Lee, S. L. Cohen, B. T. Chait, M. Li, and R. MacKinnon. 1998. Crystal structure and functional analysis of the HERG potassium channel N terminus: a eukaryotic PAS domain. *Cell.* 95:649–655.

Chiara, M. D., F. Monje, A. Castellano, and J. López-Barneo. 1999. A small domain in the N-terminus of the regulatory α-subunit Kv2.3 modulates Kv2.1 potassium channel gating. *J. Neurosci.* 19:6865–6873.

Chiesa, N., B. Rosati, A. Arcangeli, M. Olivotto, and E. Wanke. 1997. A novel role for HERG K^+ channels: spike-frequency adaptation. *J. Physiol. (Lond.).* 501:313–318.

Chouabe, C., M-D. Drici, G. Romey, J. Barhanin, and M. Lazdunski. 1998. HERG and KvLQT1/IsK, the cardiac K^+ channels involved in long QT syndromes, are targets for calcium channel blockers. *Mol. Pharmacol.* 54:695–703.

Curran, M. E., I. Splawski, K. W. Timothy, G. M. Vincent, E. D. Green, and M. T. Keating. 1995. A molecular basis for cardiac arrhythmia: HERG mutations cause long QT syndrome. *Cell.* 80:795–804.

de la Peña, P., L. M. Delgado, D. del Camino, and F. Barros. 1992. Cloning and expression of the thyrotropin-releasing hormone receptor from GH_3 rat anterior pituitary cells. *Biochem. J.* 284:891–899.

Demo, S. D., and G. Yellen. 1991. The inactivation gate of the *Shaker* K^+ channel behaves like an open-channel blocker. *Neuron.* 7:743–753.

Faravelli, L., A. Arcangeli, M. Olivotto, and E. Wanke. 1996. A HERG-like K^+ channel in rat F-11 DRG cell line: pharmacological identification and biophysical characterization. *J. Physiol. (Lond.).* 496:13–23.

Ficker, E., W. Jarolimek, J. Kiehn, A. Baumann, and A. M. Brown. 1998. Molecular determinants of dofetilide block of HERG K^+ channels. *Circ. Res.* 82:386–395.

Hancox, J. C., A. J. Levi, and H. J. Witchel. 1998. Time course and voltage dependence of expressed HERG current compared with native "rapid" delayed rectifier K current during the cardiac ventricular action potential. *Pflügers Arch.* 436:843–853.

Herzberg, I. M., M. C. Trudeau, and G. A. Robertson. 1998. Transfer of rapid inactivation and sensitivity to the class III antiarrhythmic drug E-4031 from HERG to M-eag channels. *J. Physiol. (Lond.).* 511:3–14.

Ho, S. N., H. D. Hunt, R. M. Horton, J. K. Pullen, and L. R. Pease. 1989. Site-directed mutagenesis by overlap extension using the polymerase chain reaction. *Gene.* 77:51–59.

Holmgren, M., M. E. Jurman, and G. Yellen. 1996. N-type inactivation and the S4–S5 region of the Shaker channel. *J. Gen. Physiol.* 108:195–206.

Hoshi, T., W. N. Zaggotta, and R. Aldrich. 1990. Biophysical and molecular mechanisms of *Shaker* potassium channel inactivation. *Science.* 250:533–538.

Kiehn, J., A. E. Lacerda, and A. M. Brown. 1999. Pathways of HERG inactivation. *Am. J. Physiol. Heart Circ. Physiol.* 46:H199–H210.

Kreusch, A., P. J. Pfaffinger, C. F. Stevens, and S. Choe. 1998. Crystal structure of the tetramerization domain of the Shaker potassium channel. *Nature.* 392:945–948.

London, B., M. C. Trudeau, K. P. Newton, A. K. Beyer, N. G. Copeland, D. J. Gilbert, N. A. Jenkins, C. A. Satler, and G. A. Robertson. 1997. Two isoforms of the mouse *Ether-a-go-go*-related gene coassemble to form channels with properties similar to the rapidly activating component of the cardiac delayed rectifier K^+ current. *Circ. Res.* 81:870–878.

Marten, I., and T. Hoshi. 1997. Voltage-dependent gating characteristics of the K^+ channel KAT1 depend on the N and C termini. *Proc. Natl. Acad. Sci. USA.* 94:3448–3453.

Marten, I., and T. Hoshi. 1998. The N-terminus of the K channel KAT1 controls its voltage-dependent gating by altering the membrane electric field. *Biophys. J.* 74:2953–2962.

Pascual, J. M., C-C. Shieh, G. E. Kirsch, and A. M. Brown. 1997. Contribution of the NH_2 terminus of Kv2.1 to channel activation. *Am. J. Physiol.* 273:C1849–C1858.

Rosati, B., M. Rocchetti, A. Zaza, and E. Wanke. 1998. Sulfonylurea blockade of neural and cardiac HERG channels. *FEBS Lett.* 440: 125–130.

Sanger, F., S. Nicklen, and A. R. Coulson. 1977. DNA sequencing with chain-terminating inhibitors. *Proc. Natl. Acad. Sci. USA.* 74:5463–5467.

Sanguinetti, M. C., C. Jiang, M. E. Curran, and M. T. Keating. 1995. A mechanistic link between an inherited and an acquired cardiac arrhythmia: HERG channel encodes the IK_r potassium channel. *Cell.* 81:299–307.

Sanguinetti, M. C., and Q. P. Xu. 1999. Mutations of the S4–S5 linker alter activation properties of HERG potassium channels expressed in *Xenopus* oocytes. *J. Physiol. (Lond.).* 514:667–675.

Schäfer, R., I. Wulfsen, S. Behrens, F. Weinsberg, C. K. Bauer, and J. R. Schwarz. 1999. The erg-like current in rat lactotrophs. *J. Physiol. (Lond.).* 518:401–416.

Schönherr, R., and S. H. Heinemann. 1996. Molecular determinants for activation and inactivation of HERG, a human inward rectifier potassium channel. *J. Physiol. (Lond.).* 493:635–642.

Schönherr, R., B. Rosati, S. Hehl, V. G. Rao, A. Arcangeli, M. Olivotto, and E. Wanke. 1999. Functional role of the slow activation property of ERG K^+ channels. *Eur. J. Neurosci.* 11:753–760.

Smith, P. L., T. Baukrowitz, and G. Yellen. 1996. The inward rectification mechanism of the HERG cardiac potassium channel. *Nature.* 379: 833–836.

Spector, P. S., M. E. Curran, M. T. Keating, and M. C. Sanguinetti. 1996a. Class III antiarrhythmic drugs block HERG, a human cardiac delayed rectifier K^+ channel. *Circ. Res.* 78:499–503.

Spector, P. S., M. E. Curran, A. Zou, M. T. Keating, and M. C. Sanguinetti. 1996b. Fast inactivation causes rectification of the I_{Kr} channel. *J. Gen. Physiol.* 107:611–619.

Suessbrich, H., R. Schönherr, S. H. Heinemann, B. Attali, F. Lang, and A. E. Busch. 1997a. The inhibitory effect of the antipsychotic drug haloperidol on HERG potassium channels expressed in *Xenopus* oocytes. *Br. J. Pharmacol.* 120:968–974.

Suessbrich, H., R. Schönherr, S. H. Heinemann, F. Lang, and A. E. Busch. 1997b. Specific block of cloned *Herg* channels by clofilium and its tertiary analog LY97241. *FEBS Lett.* 414:435–438.

Suessbrich, H., S. Waldeger, F. Lang, and A. E. Busch. 1996. Blockade of HERG channels expressed in *Xenopus* oocytes by the histamine antagonists terfenadine and astemizole. *FEBS Lett.* 385:77–80.

Taglialatela, M., A. Pannaccione, P. Castaldo, G. Giorgio, Z. Zhou, C. T. January, A. Genovese, G. Marone, and L. Annunziato. 1998. Molecular basis for the lack of HERG K^+ channel block-related cardiotoxicity by the H1 receptor blocker cetirizine compared with other second-generation antihistamines. *Mol. Pharmacol.* 54:113–121.

Terlau, H., S. H. Heinemann, W. Stühmer, O. Pongs, and J. Ludwig. 1997. Amino terminal-dependent gating of the potassium channel rat eag is compensated by a mutation in the S4 segment. *J. Physiol. (Lond.).* 502:537–543.

Titus, S. A., J. W. E. Warmke, and B. Ganetzky. 1997. The *Drosophila erg* K^+ channel polypeptide is encoded by the *seizure* locus. *J. Neurosci.* 17:875–881.

Trudeau, M. C., J. W. Warmke, B. Ganetzky, and G. A. Robertson. 1995. HERG, a human inward rectifier in the voltage-gated potassium channel family. *Science.* 269:92–95.

Wang, J., M. C. Trudeau, A. M. Zappia, and G. A. Robertson. 1998. Regulation of deactivation by an amino terminal domain in *Human ether-a-go-go-related gene* potassium channels. *J. Gen. Physiol.* 112: 637–647.

Wang, S., S. Liu, M. J. Morales, H. C. Strauss, and R. L. Rasmusson. 1997. A quantitative analysis of the activation and inactivation kinetics of HERG expressed in *Xenopus* oocytes. *J. Physiol. (Lond.).* 502:45–60.

Wang, X., E. R. Reynolds, P. Deak, and L. M. Hall. 1997. The *seizure* locus encodes the *Drosophila* homolog of the HERG potassium channel. *J. Neurosci.* 17:882–890.

Warmke, J. W., and B. Ganetzky. 1994. A family of potassium channel genes related to *eag* in *Drosophila* and mammals. *Proc. Natl. Acad. Sci. USA.* 91:3438–3442.

Zhou, Z., Q. Gong, B. Ye, Z. Fan, J. C. Makielski, G. A. Robertson, and C. T. January. 1998. Properties of HERG channels stably expressed in HEK 293 cells studied at physiological temperature. *Biophys. J.* 74: 230–241.